

Fundamental transport processes in ensembles of silicon quantum dots

I. Balberg, E. Savir, and J. Jedrzejewski

The Racah Institute of Physics, The Hebrew University, Jerusalem 91904, Israel

A. G. Nassiopoulou and S. Gardelis

IMEL/NCSR Demokritos, P.O. Box 60 228, Aghia Paraskevi, 153 10 Athens, Greece

(Received 13 November 2006; revised manuscript received 23 April 2007; published 27 June 2007)

For a better understanding of the physical properties of semiconductor quantum dot ensembles, we have followed the behaviors of the transport and photoluminescence above, at, and below the percolation threshold of ensembles of Si quantum dots that are embedded in a SiO_2 matrix. Our study revealed the roles of the interdot conduction, the single dot charging, and the connectivity in such systems. We conclude that while the first two determine the global transport, a connectivity dependent migration determines the coupling between the electrical and optical properties.

DOI: [10.1103/PhysRevB.75.235329](https://doi.org/10.1103/PhysRevB.75.235329)

PACS number(s): 73.63.Kv, 73.22.-f, 78.60.-b, 78.67.Hc

I. INTRODUCTION

In contrast with the many data and the understanding achieved thus far regarding the optical behavior^{1,2} [notably the photoluminescence (PL)] of single nanocrystalline semiconductor (NCSC) quantum dots, the fundamental understanding of the transport and optical response of solid-state ensembles of such dots has not emerged thus far.³⁻⁵ This is in spite of the significant forward strides that were made in the many studies of ensembles of ligand-capped semiconductor quantum dots.^{6,7} The solid ensembles consist of “touching” (but not capped or coalescing) NCSC dots that are usually in the form of composites⁸ or aggregates of touching dots.⁹ This is in contrast with arrays of “nontouching” NCSC dots¹⁰ where the experimental observations reflect essentially the contribution of the individual dots. In particular, the *interplay* between properties of the individual semiconductor nanocrystallites (NCs) at the quantum confinement regime^{1,7,11} and the connectivity of the system (which is essential for the understanding of the transport properties of the ensembles) has hardly been studied previously, and when discussed, it was mainly for ensembles of ligand-capped metallic nanoparticles.¹²

The purpose of the present work is bridging between the physics of the microscopic-quantum regime and the physics of the macroscopic-classical system. Correspondingly, we attempt to demonstrate the existence of the *basic microscopic* processes and their integrated manifestation in the transport as well as their relation to the optical processes of solid ensembles of quantum dots (QDs) by the study of ensembles of silicon nanocrystallites in the vicinity of the percolation threshold of the ensembles. Noting that such application of the percolation threshold regime has not been attempted before, we fully exploited the advantage of the cosputtering film deposition technique,^{13,14} preparing a series of samples of silicon NCs, such that each sample consists of a small increment of the fractional volume content (or density) Δx of the volume percent of the (crystalline or amorphous) silicon phase x along a rectangular substrate,¹³ and a corresponding increment Δd in the crystallites size d with respect to its preceding sample.¹⁴ In passing, we note that in contrast with the case of granular metals,¹³ this advantage has not been

fully utilized for the study of ensembles of semiconductor QDs (Ref. 15) that, as we show below, is *quite critical* for the evaluation of the local and global mechanisms that determine the effects of the above interplay on the transport. Moreover, working, in contrast with previous works,^{8,15} with a four-probe coplanar configuration, we have ensured that the results obtained have to do with “bulk” properties of the QD ensembles.

To set, however, the stage for the description of the system that we study, we recall that in granular metals,^{13,16} there are two contributing conduction routes.^{13,17} Above a certain metal grain volume content x_c , there is a “continuous” metallic network of coalescing QDs and a metallic bulk-like conduction dominates. Correspondingly, x_c is the classical percolation threshold.^{16,17} For $x < x_c$, the electron transfer between the individual grains is possible only by tunneling.^{13,17} In the latter, the so-called dielectric regime, the grains charging phenomenon^{13,18,19} (the “Coulomb blockade”) takes place and nonlinear current-voltage characteristics (I - V 's) are observed.^{12,13}

If the above considerations apply to ensembles of semiconductor QDs, one would expect that a *bona fide* universal percolation transition of the conductivity, at an x_c with a value of the order observed in granular metals,^{13,16} and a transition from linear (or slightly nonlinear in NCSC, due to the noncoalescence of crystallites which is generally different than in the case in granular metals) to nonlinear I - V 's will be observed, as the value of x is decreased through x_c . The latter is expected since, as x_c is approached from above, the conduction in the network will be determined more and more by the so-called singly connected bonds,^{16,20} i.e., by relatively isolated QDs, so that the tunneling transport and the single electron charging events may be disclosed by the I - V 's.^{7,10,13} The experimental challenge in trying to verify the latter expectations is, of course, to carry out the measurement for a sample with an x value that is as close as possible to x_c but to still have a measurable current.

Following the above considerations for ensembles of NCSC, we have prepared (by finding the proper cosputtering and postdeposition conditions) samples of silicon nanocrystallites^{14,21} that exhibit a percolation transition.^{16,20} Our results as discussed below not only elucidate the con-

duction mechanisms but also establish the so far *missing link* in the understanding of the relation between the transport and the photonic (PL) properties of such systems.

In this paper, we give only a brief account of the preparations of the samples involved in our present study as these were detailed in our previous papers.¹⁴ Similarly, the transport and phototransport measurement techniques were presented previously in related^{9,21,22} or unrelated^{16,23} studies. Here, we only emphasize then the specific details that were essential for the present work. These and the structural characterization of the samples,¹⁴ which are so important for connecting the macroscopic observations with the nanostructure of the system under study, are given in Sec. II. In Sec. III, we present our macroscopic experimental results, and in Sec. IV, we discuss them in relation to the nanostructure and the percolation model. We also emphasize there the issues associated with the understanding of the present results in more detail and our corresponding suggestions.

II. EXPERIMENTAL DETAILS

The films we deposited, usually about 1 μm thick, were fabricated by the cosputtering of Si and SiO_2 (Ref. 14) from two separate targets onto a quartz slide (13 cm long), thus utilizing the unique ability to produce a series of samples under exactly the same conditions, but with a controllable quasicontinuous set of the silicon fractional volume contents x .¹³ After the sputtering, the samples were annealed at 1150 $^\circ\text{C}$ under a nitrogen flow, yielding films that appear to be composed of two immiscible phases, one of silicon nanocrystallites and the other of an amorphous (mainly SiO_2) matrix. The important point for the present study is that the electrical and optical properties can be measured with a high ($\Delta x \approx 2$ vol %) resolution of x and a corresponding¹⁴ high resolution ($\Delta d/D \approx 0.03$) of d , where d is the average nanocrystallite diameter for a given x and where D is the d range which we have along the substrate slide. In our typical samples the d values were between 3 and 8 nm (i.e., $D = 5$ nm) for x values between 10 and 80 vol %.¹⁴ For the electrical measurements, we have sputtered 1-mm-wide Al (or Ag) contacts with a spacing of about 1 mm. It is important to note that in our study, the following *measures were taken* to ensure that the electrical contacts or the electrical setup do not play any role in the measured currents. First, the measurements were carried out in a coplanar configuration so that the resistance of the bulk was much larger than that of the contacts. The latter was verified by the fact that the measured resistance was found to scale with the interelectrode spacing and that no difference was found between the results obtained in two-probe and four-probe configurations and/or when we have exchanged one or two of the coplanar Al contacts with In contacts. Second, to ensure that no spurious coupling between the measurement apparatus and the sample takes place, independent transport measurements were conducted on similarly prepared samples using two very different experimental apparatuses.^{22,23} From all these tests, we safely conclude that the measured currents are determined by the bulk resistance of the samples (the corresponding film sections around a given x) that are 1 mm long and have a

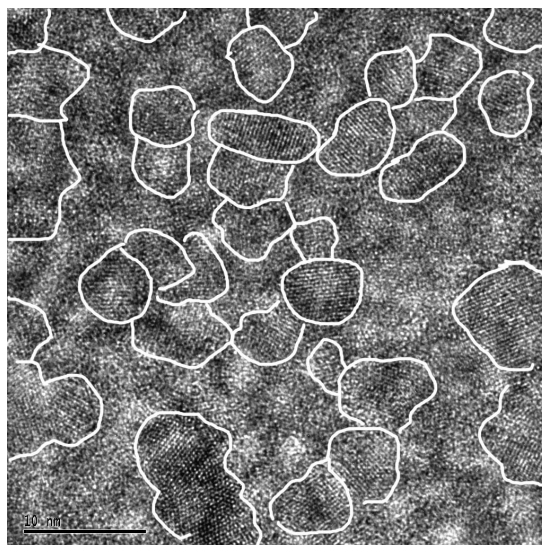


FIG. 1. HRTEM micrograph of a sample of 80 vol % silicon and 20 vol % SiO_2 . The silicon nanocrystallites that are identified by the silicon crystal planes are marked by their borders. The rest of the micrograph appears to represent the noncrystalline Si or SiO_2 islands.

cross section for transport of $3 \times 10^{-3} \text{ mm}^2$. Moreover, this configuration eliminates possible high-field effects that may be involved in the transport and the PL. The photoconductivity was measured by exposing the area between the contacts ($1 \times 3 \text{ mm}^2$) to a He-Ne laser (633 nm, flux of 70 mW/cm^2),²³ while the PL was measured between pairs of coplanar contacts by applying an Ar-ion laser (488 nm, flux of 10 W/cm^2). The latter PL measurements and the analysis of the results that were obtained in various temperatures have been described in great detail previously,¹⁴ showing, in particular, the expected quantum confinement relation between the size of the particles and the photon energy at which the PL has its peak. All the measurements reported here, however, were carried out at room temperature.

To characterize our system of nanocrystallites embedded in a SiO_2 matrix, we obtained images of high-resolution transmission electron microscopy (HRTEM).¹⁴ In Fig. 1, we show HRTEM taken at $x \approx 80$ vol %. The silicon crystal planes disclose the NCs (encircled by white loops). The other areas in the image, i.e., the noncrystalline areas, consist of amorphous silicon and/or SiO_2 glass areas.²⁴ Following the fact that our HRTEM images of the low x ($x < 20$ vol %) regime have revealed isolated spherical nanocrystallites,¹⁴ the present images suggest that as the percolation threshold of touching crystallites, x_c , is approached from above, the NC network becomes sparse and isolated crystallites become the tunneling bridges or the singly connected bonds²⁰ between various parts of the percolation backbone.

III. EXPERIMENTAL RESULTS

Turning to the results of the conductivity and photoconductivity measurements, we see in Fig. 2 that their depen-

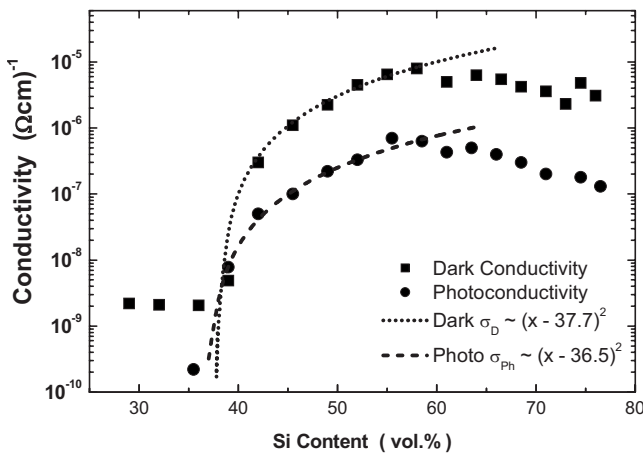


FIG. 2. The dependence of the dark conductivity and the photoconductivity on the silicon content in a typical cosputtered film. For this film, there is a sample at $x=39$ vol % silicon that is very close to the percolation threshold but still has a measurable conductivity.

dence on x can be well fitted by the theoretical percolation behavior of $\sigma \propto (x-x_c)^t$, where t was found to be very close to the *universal*^{20,25} value of 2. This behavior (of $t \approx 2$) was verified on many series of samples by the best fit of the corresponding log-log plots using the procedures that we applied previously to other systems.²⁶ The only essential difference that we found for films prepared under different conditions was the value of their x_c . These values in our many samples were in the 25–50 vol % range (as in granular metals^{13,16}). For example, for the data shown in Fig. 2, the t value was determined to be 2.1 ± 0.2 and the value of x_c was determined to be 38 ± 1 vol %. One should note, however, that in the present work, our purpose was not the determination of a very accurate value for t , as we did in Ref. 26, but rather to establish that we have a *bona fide* percolation network in order to lay the basis for the interpretation of the following experimental results.

While such confirmation of percolation theory have been given previously for various composites,^{9,13,16,26} we are not aware of such fits for NCSC systems in the *quantum confinement regime*. In particular, this has not been done for photoexcited carriers in this regime, and the similar simultaneous percolation behavior of both kinds of conductivity has not been demonstrated. In fact, the application of the photoconductivity to quantitatively characterize the percolation behavior is quite rare though it has been done, for example, on a system of dye-sensitized TiO₂ films in which the TiO₂ crystallites have a diameter of 19 nm.²⁷ The confirmation of the percolation behavior is of importance here in order to establish that, with the additional consideration of the images shown in Fig. 1, we have a genuine percolation transition around which we can study the so far unstudied properties of the “dielectric-like” regime¹³ in a system of semiconductor quantum dots. In the present context, the similar dependence of the conductivity and photoconductivity means that this dependence is not determined by the carrier concentration but rather by their interdot “mobility” and the network connectivity. As explained above, we were interested in ap-

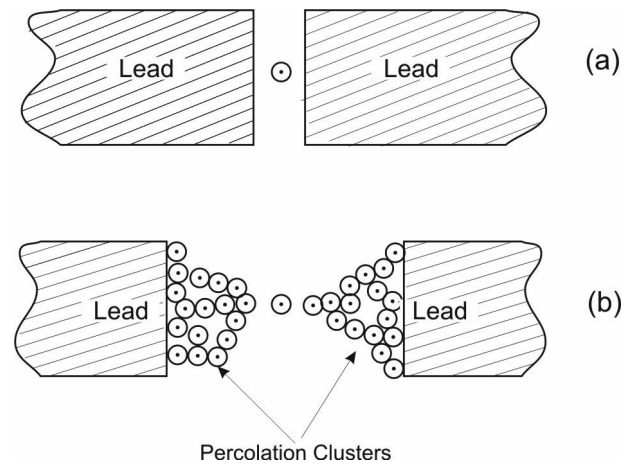


FIG. 3. An illustration of (a) a DBTJ and (b) the expected “critical crystallite” DBTJ (a singly connected bond in the present percolation networks) which connects, by “sequential” tunneling, larger parts of the system.

proaching the percolation threshold as close as possible with the hope to correlate the macroscopically measured I - V characteristics with the local intercrystallite conduction mechanism. The way we expected this to happen is presented in Fig. 3. This figure illustrates that, from the percolation connectivity point of view, the QD in Fig. 3(b) is a singly connected bond,^{20,25} while from the local-physical behavior point of view, it yields the double barrier tunnel junction^{7,10} (DBTJ) configuration that is illustrated in Fig. 3(a).

The behavior expected following the illustration of Fig. 3 was confirmed by the most significant feature of the I - V characteristics that we found in the threshold regime, i.e., the existence of a “voltage gap” that does not exist in the “above-threshold” regime. This bias gap, as shown in Fig. 4, is *clearly reminiscent of the observations in a single DBTJ* of a semiconductor quantum dot.^{7,10} In principle, the observed bias gap for x in the vicinity of x_c can be associated with resonant tunneling and/or a Coulomb blockade.^{7,28} While there are only very few works in which the first mechanism appears to be present in a system of silicon nanocrystallites,^{29,30} there are numerous results that support the presence of the latter mechanism, at least in small or dilute ensembles of silicon nanocrystallites.^{22,31–35} In fact, the comparison of the present results with the many results obtained on two-dimensional arrays of Si NCs or on a collection of a few QDs, which have been attributed to a simple sum of single dot charging events and that have disclosed^{10,22,35} a *bias gap of the order found here*, further indicates that the latter gap is dominated by a “Coulomb gap” phenomenon that is associated with very few QDs, as suggested by the model given in Fig. 3. Of course, the real Coulomb gap value is smaller than the observed bias gap since the latter is due to the voltage distribution in the “leads” [see Fig. 3(b)] and in the DBTJ.^{7,28}

In order to get an independent evidence that in our samples we are dealing mainly with a Coulomb-gap-like charging effect, we have prepared samples as above, but on conducting silicon substrates. This, perpendicular to the film, “vertical” configuration enables the measurement of the

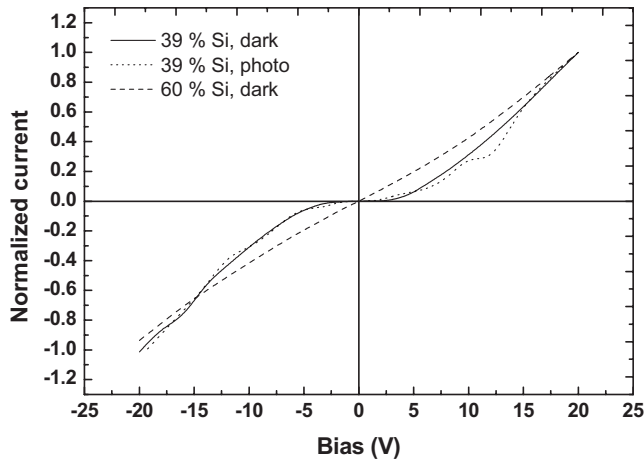


FIG. 4. Normalized (at 20 V) current-voltage characteristic of a sample with $x=60$ vol % silicon (dashed curve) and current-voltage and photocurrent-voltage characteristics of the sample with $x=39$ vol % silicon (solid and dotted curves). These samples belong to the series of samples the conductivity “profile” of which was shown in Fig. 2. The value of 1 corresponds to 51 nA for the first sample and 2 nA for the dark current and 0.16 nA for the photocurrent of the latter sample.

capacitance-voltage (C - V) characteristics^{22,36,37} on these samples. Using an “upper” Hg electrode and the silicon substrated films, Antonova *et al.*³⁸ have found on our samples that there was hardly measurable stored charge for the x regime above [$x > (x_c + 3)$ vol %] and “far” below [$x < (x_c - 14)$ vol %] the percolation threshold that was in this case at $x_c = 34$ vol %. There was, however, an appreciable charge stored, at, and in the region close below x_c . The peak of the stored charge was found at $x = (x_c - 8)$ vol %. The percolation threshold was identified in that vertical configuration by a sharp drop in the macroscopic resistance perpendicular to the film. Considering these results and comparison with the above-mentioned results on the charging effects,^{22,31,32,35} there is very little doubt left that the behavior shown in Fig. 4 is associated with the charging of the “singly connected” nanocrystallites around the percolation threshold. In passing, we note that while the C - V measurements are very useful for the determination of the charge stored in various semiconductor systems,^{36,37} the corresponding “two terminal” configuration, as explained above, does not allow the proper evaluation of the bulk transport mechanism due to the possible contribution of contact effects.

Turning to our study of the relation between the PL and the transport properties, we prepared a ten times thicker (10 μm) film than in the above-discussed samples (and in the samples that we have studied intensively before¹⁴), allowing us to follow the PL dependence of x as close as possible to x_c . To appreciate this observation, we plot in Fig. 5 the peak PL intensity as a function of x for various photon energies. Noting that for the observed spectral range the spectrum is associated with the quantum confinement regime,^{2,4,39} each photon-energy represents a particular value of d . That the latter is the case in our samples is well borne out by the monotonic correlation that we found previously¹⁴ between the peak energy of the PL spectra of a sample, of a

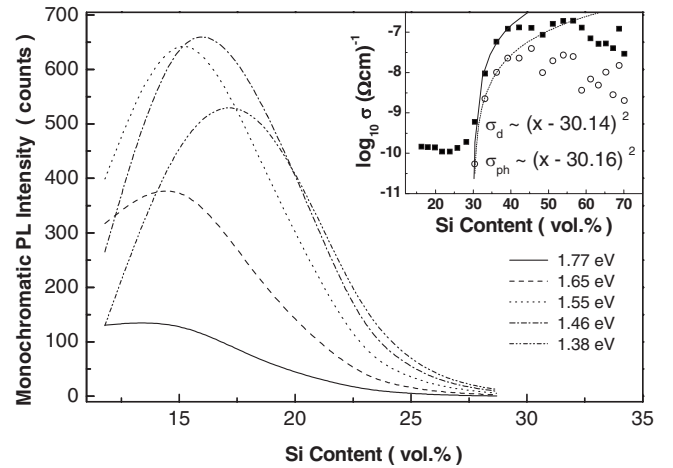


FIG. 5. The typical photoluminescence peak intensity for various photon energies as a function of the silicon volume content. In the inset, we show the corresponding dependence of the dark conductivity (full squares) and the photoconductivity (open circles) on the silicon content as well as the fitted curves to the prediction of percolation theory.

given x , with the center of the distribution of its crystallite diameters. In the inset of Fig. 5, we show the percolation behavior of the conductivity and photoconductivity in the present particular sample. It is clearly seen that these transport properties and the PL are *exclusive*. Studying many films that were prepared under different conditions, we found that while there may be some overlap between the conductivity “tail” and the PL tail, there is never such an overlap between the PL and the photoconductivity tail, i.e., the latter two are completely exclusive (see below).

The most conspicuous observation in Fig. 5 is the three orders of magnitude rise and decay of the PL with x . Combining this observed decay, as x approaches x_c from below, with the increasing dispersive nature of the PL that we found previously¹⁴ [by time resolved PL (TRPL)], we associate the two phenomena with the increasing probability of the optically generated carriers to migrate to the environment of the isolated QD in which these carriers were generated. Such a mechanism has been proposed originally (solely on the basis of TRPL) for porous silicon⁴⁰ and later for ensembles of Si QDs.⁴¹ Here, however, following the observed percolation behavior of the photoconductivity, we apply percolation theory from which we know^{20,21} that finite clusters of touching QDs [see Fig. 3(b)] grow sharply and appreciably in a universal manner as x increases toward x_c . This can be appreciated semiquantitatively by considering the fact that the average cluster size increases from d (say, at $x=0$, see HR-TEM images in Ref. 14) to $d[(x_c - x)/x_c]^{-\nu}$ [where $\nu=0.88$ (Ref. 20)] as x approaches x_c from below. This will be here from about $3d$ at $x=20$ vol % to about $10d$ at $x=27$ vol %. The corresponding increase will yield then a much larger probability for the separation of the *a priori* quantum confined photoexcited electron-hole pairs and, thus a much weaker radiative recombination (i.e., a weaker PL). The way we present our PL data in Fig. 5 helps to appreciate this argument as follows. In this figure, we see that for low x values, the increase of the PL with x depends strongly on d

(noting that each photon energy represents a given crystallite size d , see above), while for the higher x values (all still in the $x < x_c$ regime), the decay of the PL with x appears to follow a universal-like (d -independent) behavior. Now, the initial rise of the PL with x is well understood in terms of the increase of the concentration of the QDs with x , since the preference of the various QD concentrations is determined by the combination of the preparation parameters (mainly annealing²⁴ and oxidation) and the value of x . On the other hand, our observation of a universal-like decrease of the PL with x dominates over the effect of the particular d values (in our corresponding 3–6 nm d range, see above). Such a behavior is well in accord with the expected strong universal increase^{20,21} of the size of the finite (connected crystallites) clusters as x approaches x_c from below, implying also an increasing universal-like migration probability with increasing x . The latter thus overshadows possible milder d -dependent effects.¹⁴ The association of the above drop of the PL with the increase in the cluster size (for $x < x_c$) is well supported by the above-mentioned peak in the stored charge below x_c , since as x_c is approached from below, the carriers migration within the larger cluster facilitates their motion to the contacts within the time of the transport measurement, on one hand, and the separation of the electron-hole pair from the confined crystallite volume in which they were generated, within the time of the radiative recombination, on the other hand.

The above-mentioned *general and complete exclusion of the photoconductivity and the PL* is well understood then by our above-suggested migration model as due to the competition between the short enough radiative recombination time that is induced by the quantum confinement³⁹ (reflected by the high PL intensity) and the migration-nonradiative recombination^{40,41} (reflected by the magnitude of the photoconductivity). The latter overcomes the former as the probability for migration increases, i.e., as the QD clusters grow, when the percolation threshold is approached.

IV. DISCUSSION

In the work reported in this paper, we have examined the effect of the connectivity, in ensembles of semiconductor quantum dots, on the transport and optical response of the corresponding systems. In these systems, the local connectivity is determined by the tunneling of charge carriers between adjacent nanocrystallites similar to the case encountered in granular metals in the dielectric regime.^{13,16–18} Correspondingly, the closer the semiconductor quantum dots to each other (that follows the increase in their concentration), the larger the distance to which the charge carrier can wander from the individual crystallite at which it was (thermally, optically, or electrically) excited. In other words, the tunneling-connected^{16,25} quantum dot clusters grow in size with the increase of their concentration, as predicted by percolation theory.^{16,20} This growth proceeds until at a certain concentration, the percolation threshold x_c , an infinite cluster forms. It is apparent then that upon the increase of the cluster sizes, a “delocalization”⁴² of the carrier from its confinement in the individual quantum dot to larger regions of the en-

semble will take place, i.e., the charge carrier will belong to a cluster of quantum dots rather than to an individual quantum dot. This, in turn, will also yield a corresponding decrease in the local charging energy in comparison with that of the single isolated dot.

In the present work, we essentially followed the effect of this delocalization on both the electrical and optical properties that we found to be well correlated as follows. As long as the clusters are small enough, they “keep” the carrier that resides in them and become charged when an excess charge carrier reaches them, as in the well-known cases of granular metals¹³ and single semiconductor quantum dots.⁷ As in those cases, transport through the system can take place only if a corresponding charging (or Coulomb) energy is provided. If this energy is provided electrically, a “bias gap” is observed.⁷ Once there is no confined charge, or the single electronic charge is spread over a large cluster, the diminishing charging energy is followed by the shrinking of the bias gap. In particular, above the percolation threshold, the charge carriers can reach the electrodes more readily and no bias gap is expected. The results shown in Fig. 4 are well in accordance with this physical picture. Comparison of these results with the expectations that follow Fig. 3 further confirms our suggestion that one can mimic the microscopic double barrier tunnel junction using a macroscopic system by taking advantage of the possible “isolation” of the single-quantum-dot-like effects close to the percolation threshold. This was, of course, possible here by carefully using a coplanar configuration that has enabled us to reliably evaluate the transport properties of the bulk, rather than the more commonly used^{8,10,43–46} vertical configuration in which the experimental findings may reflect a mixture of bulk and contact contributions.

Turning to the optical properties, we know that the electron-hole pairs are generated by the illumination in the semiconductor quantum dots. If a dot belongs to a cluster, the probability of recombination of a pair generated in it decreases with the increase of the cluster size, since the confinement of the two carriers is eliminated. Correspondingly, the increase in the connectivity, and thus in the electrical conductivity of the ensemble (that follows the increase in the concentration of the quantum dots), will be accompanied by the decrease of the probability for the radiative electron-hole recombination events. Following the above physical picture, this trend is accompanied by the decrease of the stored charge in the bulk of the system as well as by the increase in the transport via the systems. In other words, the PL and the transport will be mutually exclusive. Indeed, the results shown in Fig. 5 account well for this expectation.

The above, rather simple, picture of the effect of the connectivity on the transport and the light emission, which was the concern of the present work, provides, however, only the very gross fundamental basis for the discussion of the transport in ensembles of semiconductor quantum dots, beyond the quite well understood transport via the individual quantum dot.⁷ In what follows, we briefly review then some relevant issues that need to be resolved (and the current difficulties in resolving them) in order to get a more detailed understanding of the results shown in Sec. III.

The first and foremost difficulty that one encounters in trying to quantitatively account for the results shown in Figs.

2 and 4 is that there is, at present, no acceptable picture concerning the details of the transport mechanism in dilute systems of Si quantum dots (say, similar to the model of the dielectric regime in granular metals¹³). This is in spite of the numerous papers that have discussed this subject.^{8,43–46} This situation appears to be a result of the experimental and theoretical difficulties in performing and interpreting the results of the most straightforward tool for the evaluation of the transport mechanism, i.e., the temperature dependence of the electrical conductivity, $\sigma(T)$. The very high resistance of the corresponding samples does not enable such measurements in the coplanar configuration (of the type we use here), and almost all the reported $\sigma(T)$ measurements were carried out in the vertical (perpendicular to the film surface) configuration. This, as pointed out in Secs. I and II, yields a mixture of bulk and contact effects. Moreover, even in the vertical configuration, the range of the temperatures used was usually too narrow for the derivation of reliable $\sigma(T)$ power-law dependencies that may shed light on the transport mechanism.

On the theoretical end, one notices that even for the much simpler system of granular metals¹³ that provides a simple basic reference for the transport in semiconductor quantum dots,⁶ there is still an ongoing controversy regarding the interpretation of the $\sigma(T)$ dependence.^{18,47–49} For example, tunneling via optimal paths under Coulomb blockade and hopping in a disordered system are predicted to have similar $\sigma(T)$ dependencies that do not enable a unique interpretation of such data. This, of course, further aggravates the complications that are added when one considers semiconductor quantum dots. In the latter system, there are the additional effects of level quantization and resonant tunneling,^{29,30,50} the possible contribution of interparticle interfaces⁵¹ and, most importantly, the source of the charge carriers and the corresponding carrier statistics remain unspecified. In fact, there were so far only very few attempts that considered this problem.⁵² Usually, the $\sigma(T)$ results are discussed in terms of a specific charge-transfer mechanism (say, hopping), but there is usually no account of the entities between which the hops take place (e.g., defects, surfaces, and quantum dots), the energy levels that are involved (e.g., in the quantum dot^{44,52,53} as suggested in other quantum dot ensembles⁵⁴), and the origin of the carriers that do the hops. It is not surprising then that so many transport mechanisms have been suggested in order to interpret the various data on the transport in ensembles of Si quantum dots by different authors. These include thermal emission,⁴⁴ tunneling through barriers,⁴⁵ tunneling under Coulomb blockade,⁵² various kinds of hopping,^{43,46} and space-charge transport.⁸

In contrast, it is well known that the current-voltage characteristics that are associated with single semiconductor nanocrystallites show very clearly that the transport through those crystallites is controlled by tunneling and by Coulomb blockade effects.⁷ Correspondingly, while recognizing the fact that the details of the transport mechanisms, in ensembles of silicon nanocrystallites, are not established yet, the basis given by the latter effects and the strong evidence for tunneling (or various hopping) processes and charging events in dilute ensembles of silicon quantum dots^{10,22,34,35} enable us to discuss our results within the framework of se-

quential tunneling under Coulomb blockade conditions,¹⁰ as we have done in the present work. At present, it appears then that one would need evidence beyond the $\sigma(T)$ dependence to reliably establish the transport mechanisms in ensembles of silicon quantum dots beyond the above general framework. Such support can come mainly from local probe microscopy^{7,9} or from additional experimental methods that address particular aspects of the problem.⁵⁵ In the present work, we overcome one of these aspects by showing the same behavior of the conductivity and photoconductivity, thus suggesting that the carriers in the system originate from the nanocrystallites. An extension of such a study can further enable to separate mobility and carrier concentration effects, as we demonstrated recently for ensembles of CdSe quantum dots.⁵⁴

The other important issue concerning our present paper is the relation between the bias gap found in Fig. 3 and the microscopic Coulomb (charging) energies expected^{7,13,56} in the system. While we have previously considered some aspects of the charging effects and tunneling in a chain of nanoparticles⁵⁶ following the simple Sheng model,¹³ we realize that a quantitative theoretical consideration of the present system requires quite an elaborate theory or simulation. This is so, even though the basic physics is as outlined above, i.e., the observed bias gap is the sum of the voltage drop across the large (“almost percolating”) clusters [see Fig. 3(b)], which are the leads to the single quantum dot (or a small set¹⁰ of such dots) that is charged, and the Coulomb energy of the latter. The Coulomb energy is of the order of a tenth of an eV.^{7,10,56} To correspondingly account then quantitatively for the observed bias gap is not straightforward even for the single quantum dot,^{10,28} the triple junction is more complicated,⁵⁷ and our case of a multijunction has not even been attempted thus far. While very crude models exist,^{10,56} in a more detailed model, one will have to consider nontrivial routes (in which the Coulomb blockade may or may not play some role), more specifics of the tunneling mechanism (tunneling probabilities), and the variations in the tunneling barrier widths and heights as well as the dot sizes along the current path. Here, it appears that local probe microscopies^{7,9,58} or the use of controllable small ensemble^{10,59,60} can provide essential parameters, with which one can try and fit possible models for this rather complicated system of solid ensembles of semiconductor quantum dots.

The third central issue is the interpretation of the PL decay characteristics in Fig. 5 in terms of the present, migration within a cluster of quantum dots, model. We first note that while the previous works that have considered the nonradiative recombination^{14,40,41} are related in many ways to the model suggested here, their picture is based on “migration” to the surface or the interface with an adjacent quantum dot, while in the present study, we suggest quite a different model that is associated with a transport process that enables the *electron-hole separation within a cluster*, where the size of the latter follows the predictions of percolation theory.²⁰ We note that, in general, the problem of the PL decay with x has hardly been considered previously and that the finding of the common (d -independent) PL decay (with x) characteristics is in accord with the universal increase of the average cluster

size and, thus, can be used as a guide concerning the dominant process in models that will try to account for this decay. However, the development of an appropriate quasiquantitative model for the observed behavior will have to take into account the tunneling probabilities and the radiative and non-radiative recombination probabilities (or decay times^{14,39}) that are involved in the recombination processes. Again, such models, when available, will have to be compared with (the already available⁵⁸) various measurements on a single dot or a small cluster of quantum dots. Also, using, in addition to the present sample configuration, a vertical configuration by which high fields can be applied and yield a pair separation seems promising for a more quantitative account of the relation between local transport and carrier recombination.⁶¹ On the theoretical end, a possible starting point may be the consideration of the recombination processes in ensembles⁵ and coupling that with the above-mentioned information on the clusters (that is determined by the concentration of the dots) and with the percolation-tunneling models.²⁵ The qualitative picture that we can derive at present is based on the competition mechanism that we suggested. This mechanism, as noted above, explains well our observations. Of course, as we noted above, for a more detailed and/or quantitative discussion, one should involve not only the percolation statistics that we considered here but also the additional parameters of the tunneling and the efficiencies of the radiative and non-radiative processes.

We see then that for both the electrical and the optical properties, further theoretical developments are required in

order to quantitatively account for the observed behavior of these properties beyond the theory of the single semiconductor quantum dot and beyond the qualitative physical picture that we derived above. It also appears that, on the experimental end, local probe spectroscopies and their application to small isolated clusters of variable sizes can indicate the approximations that can be made when one considers macroscopic ensembles. On the other hand, the present work has shown, as concluded below, that the basic microscopic processes can be studied on a macroscopic system if it provides the special network that one encounters around the corresponding percolation threshold.

In conclusion, in this paper, we presented two phenomena around the percolation transition in ensembles that consist of semiconductor quantum dots. Following these findings, we are now able to suggest the basic physical mechanisms that dominate the transport behavior of quantum dot solid ensembles below (migration), at (Coulomb blockade), and above (tunneling) their percolation threshold.

ACKNOWLEDGMENTS

This work was supported in part by the Israel Science Foundation and in part by the Israeli Ministry of Science. The authors would like to thank Y. Goldstein and O. Millo for very helpful discussions and I. Popov for carrying out the HRTEM measurements. I.B. would like to acknowledge the funding support of the Enrique Berman chair in Solar Energy Research at the HU.

¹S. V. Gaponenko, *Optical Properties of Semiconductor Nanocrystals* (Cambridge University Press, Cambridge, 1998).

²*Light Emission in Silicon: From Physics to Devices*, edited by D. J. Lockwood (Academic, New York, 1998).

³Y. Yoffe, *Adv. Phys.* **50**, 1 (2001).

⁴O. Bissi, S. Ossicini, and L. Pavesi, *Surf. Sci. Rep.* **38**, 1 (2000).

⁵See, for example, M. V. Artemyev, U. Woggon, H. Jaschinski, L. I. Gurinovich, and S. V. Gaponenko, *J. Phys. Chem. B* **104**, 11617 (2000).

⁶For a review, see D. Vanmaekelbergh and P. Liljeroth, *Chem. Soc. Rev.* **34**, 299 (2005); see also N. Y. Morgan, C. A. Leatherdale, M. Drndić, M. V. Jarosz, M. A. Kastner, and M. Bawendi, *Phys. Rev. B* **66**, 075339 (2002); D. Yu, C. J. Wang, B. L. Wehrenberg, and P. Guyot-Sionnest, *Phys. Rev. Lett.* **92**, 216802 (2004); D. V. Talapin and C. B. Murray, *Science* **310**, 86 (2005).

⁷U. Banin and O. Millo, *Annu. Rev. Phys. Chem.* **54**, 465 (2003).

⁸T. A. Burr, A. A. Seraphin, E. Werwa, and K. D. Kolenbrander, *Phys. Rev. B* **56**, 4818 (1997).

⁹D. Toker, I. Balberg, O. Zelaya-Angel, E. Savir, and O. Millo, *Phys. Rev. B* **73**, 045317 (2006).

¹⁰See, for example, Y. Inoue, A. Tanaka, M. Fujii, S. Hayashi, and K. Yamamoto, *J. Appl. Phys.* **86**, 3199 (1999); M. Shalchian, J. Grisolia, G. Ben Assayag, H. Coffin, S. M. Atarodi, and A. Claverie, *Solid-State Electron.* **49**, 1198 (2005).

¹¹L. Banyai and S. W. Koch, *Semiconductor Quantum Dots* (World Scientific, Singapore, 1993); for silicon QDs, see N. A. Hill and

K. B. Whaley, *J. Electron. Mater.* **25**, 269 (1996).

¹²Y. Sugunuma and A. A. Dirani, *J. Phys. Chem. B* **109**, 15396 (2005), and references therein.

¹³For a review, see B. Abeles, P. Sheng, M. D. Coutts, and Y. Arie, *Adv. Phys.* **24**, 407 (1975); see, in particular, B. Abeles, H. L. Pinch, and J. I. Gittleman, *Phys. Rev. Lett.* **35**, 247 (1975).

¹⁴M. Dovrat, Y. Goshen, J. Jedrzejewski, I. Balberg, and A. Sa'ar, *Phys. Rev. B* **69**, 155311 (2004); A. Sa'ar, Y. Reichman, M. Dovrat, D. Krapf, J. Jedrzejewski, and I. Balberg, *Nano Lett.* **5**, 2443 (2005); M. Dovrat, Y. Goshen, I. Popov, J. Jedrzejewski, I. Balberg, and A. Sa'ar, *Phys. Status Solidi C* **2**, 3440 (2005).

¹⁵K. Kim, *Phys. Rev. B* **57**, 13072 (1998).

¹⁶I. Balberg, D. Azulay, D. Toker, and O. Millo, *Int. J. Mod. Phys. B* **18**, 2091 (2004).

¹⁷L. F. Fonseca and I. Balberg, *Phys. Rev. B* **48**, 14915 (1993).

¹⁸For a recent review, see I. P. Zvyagin and R. Keiper, *Philos. Mag. B* **81**, 997 (2001).

¹⁹M. A. Kastner, *Rev. Mod. Phys.* **64**, 849 (1992).

²⁰D. Stauffer and A. Aharony, *Introduction to Percolation Theory* (Taylor & Francis, London, 1992).

²¹I. Balberg, E. Savir, and J. Jedrzejewski, *J. Non-Cryst. Solids* **338-340**, 102 (2004).

²²A. G. Nassiopoulou, *Encyclopedia of Nanoscience and Nanotechnology* (American Scientific, Valencia, CA), Vol. 9, p. 793; A. Salonidou, A. G. Nassiopoulou, K. Giannakopoulos, A. Travlos, V. Ioannou-Souglideridis, and E. Tsoi, *Nanotechnology* **15**, 1

- (2004).
- ²³I. Balberg, Y. Dover, R. Naidis, J. P. Conde, and V. Chu, *Phys. Rev. B* **69**, 035203 (2004).
- ²⁴Y. Liu, T. P. Chen, Y. Q. Fu, M. S. Tse, J. H. Hsieh, and Y. C. Liu, *J. Phys. D* **36**, L97 (2003).
- ²⁵C. Grimaldi and I. Balberg, *Phys. Rev. Lett.* **96**, 066602 (2006), and references therein.
- ²⁶Z. Rubin, S. A. Sunshine, M. B. Heaney, I. Bloom, and I. Balberg, *Phys. Rev. B* **59**, 12196 (1999).
- ²⁷K. D. Benkstien, N. Kopidakis, J. van de Lagemaat, and A. J. Frank, *J. Phys. Chem. B* **107**, 7759 (2003).
- ²⁸*Single Electron Tunneling*, edited by H. Grabert and M. H. Devoret (Plenum, New York, 1991).
- ²⁹L. Tsybeskov, G. F. Grom, R. Krishnan, L. Montes, P. M. Fauchett, D. Kovalev, J. Diener, V. Timoshenko, F. Koch, J. P. McCaffrey, J.-M. Baribeau, G. I. Sproule, D. J. Lockwood, Y. M. Niquet, C. Delerue, and G. Allan, *Europhys. Lett.* **55**, 552 (2001).
- ³⁰Q.-y. Ye, R. Tsu, and E. H. Nicollian, *Phys. Rev. B* **44**, 1806 (1991).
- ³¹E. Kapetanakis, P. Normand, D. Tsoukalas, K. Beltsios, J. Stoenenos, C. Zhang, and J. van den Berg, *Appl. Phys. Lett.* **77**, 3450 (2000).
- ³²J. Shi, L. Wu, X. Huang, J. Liu, Z. Ma, W. Li, X. Li, J. Xu, D. Wu, A. Li, and K. Chen, *Solid State Commun.* **123**, 437 (2002).
- ³³S. Huang, S. Banerjee, R. T. Tung, and S. Oda, *J. Appl. Phys.* **93**, 576 (2003); M. A. Salem, H. Mizuta, and S. Oda, *Appl. Phys. Lett.* **85**, 3262 (2004).
- ³⁴E. A. Boer, M. L. Brongersma, and H. A. Atwater, *Appl. Phys. Lett.* **79**, 791 (2001); R. J. Walters, G. I. Bourianoff, and H. A. Atwater, *Nat. Mater.* **4**, 143 (2004).
- ³⁵S.-H. Choi and R. G. Elliman, *Appl. Phys. Lett.* **75**, 968 (1999); J. De la Torre, A. Souifi, M. Lemiti, A. Poncet, C. Busseret, G. Guillot, G. Brermond, O. Gonzalez, B. Garrido, and J. R. Morante, *Physica E (Amsterdam)* **17**, 604 (2003).
- ³⁶S. M. Sze, *Physics of Semiconductor Devices* (Wiley Interscience, New York, 1981).
- ³⁷E. N. Nicolian and J. R. Brews, *MOS (Metal Oxide Semiconductor) Physics and Technology* (Wiley, New York, 1981).
- ³⁸I. V. Antonova, M. B. Gulyaev, Z. S. Yenoviskaya, Y. Goldstein, and J. Jedzowski, in *Physics of Semiconductors*, edited by W. Jantsch and F. Schaffler, AIP Conf. Proc. No. 893 (AIP, Melville, NY, 2007), p. 785.
- ³⁹M. V. Wolkin, J. Jorne, P. M. Fauchet, G. Allan, and C. Delerue, *Phys. Rev. Lett.* **82**, 197 (1999).
- ⁴⁰L. Pavesi, *J. Appl. Phys.* **80**, 216 (1996).
- ⁴¹J. Heitmann, F. Muller, L. Yi, M. Zacharias, D. Kovalev, and F. Eichhorn, *Phys. Rev. B* **69**, 195309 (2004).
- ⁴²R. Zallen, *The Physics of Amorphous Solids* (Wiley, New York, 1983).
- ⁴³M. Fujii, Y. Inoue, S. Hayashi, and K. Yamamoto, *Appl. Phys. Lett.* **68**, 3749 (1996).
- ⁴⁴S. Lombardo, S. Coffa, C. Bongiorno, C. Spinella, E. Castagna, A. Sciuto, C. Gerardi, F. Ferrari, B. Fazio, and S. Privitera, *Mater. Sci. Eng., B* **69**, 295 (2000).
- ⁴⁵G. Y. Hu, R. F. O'Connell, Y. L. He, and M. B. Yu, *J. Appl. Phys.* **78**, 3945 (1995).
- ⁴⁶M. A. Rafiq, Y. Tsuchiya, H. Mizuta, S. Oda, S. Uno, Z. A. K. Durnani, and W. I. Milne, *J. Appl. Phys.* **100**, 014303 (2006).
- ⁴⁷G. A. Levin, *Phys. Lett. A* **142**, 405 (1989).
- ⁴⁸P. Sheng and J. Klafter, *Phys. Rev. B* **27**, 2583 (1983).
- ⁴⁹A. Altland, L. I. Glazman, and A. Kamenev, *Phys. Rev. Lett.* **92**, 026801 (2004); I. S. Beloborodov, A. V. Lopatin, and V. M. Vinokur, *Phys. Rev. B* **72**, 125121 (2005).
- ⁵⁰Y. Inoue, A. Tanaka, M. Fujii, S. Hayashi, and K. Yamamoto, *J. Appl. Phys.* **86**, 3199 (1999).
- ⁵¹N. Daldosso, M. Luppi, S. Ossicini, E. Degoli, R. Magri, G. Dalba, P. Fornasini, R. Grisenti, F. Rocca, L. Pavesi, S. Boninelli, F. Priolo, C. Spinella, and F. Iacona, *Phys. Rev. B* **68**, 085327 (2003).
- ⁵²M. Fujii, O. Mamezaki, S. Hayashi, and K. Yamamoto, *J. Appl. Phys.* **83**, 1507 (1998).
- ⁵³Y. Shi, X. L. Yuan, J. Wu, H. M. Bu, H. G. Yang, P. Han, Y. D. Zheng, and T. Hiramoto, *Superlattices Microstruct.* **28**, 387 (2000).
- ⁵⁴I. Balberg, E. Savir, Y. Dover, O. Portillo Moreno, R. Lozada-Morales, and O. Zelaya-Angel, *Phys. Rev. B* **75**, 153301 (2007).
- ⁵⁵B. Hamilton, J. Jacobs, D. A. Hill, R. F. Pettifer, D. Teehan, and L. T. Canham, *Nature (London)* **393**, 443 (1998).
- ⁵⁶M. R. Reshotko, A. Sa'ar, and I. Balberg, *Phys. Status Solidi A* **197**, 113 (2003).
- ⁵⁷E. Bar-Sadeh, Y. Goldstein, C. Zhang, H. Deng, B. Abeles, and O. Millo, *Phys. Rev. B* **50**, 8961 (1994).
- ⁵⁸I. Sychugov, R. Juhasz, J. Valenta, and J. Linnros, *Phys. Rev. Lett.* **94**, 087405 (2005), and references therein.
- ⁵⁹S. Banerjee, M. A. Salem, and S. Oda, *Appl. Phys. Lett.* **83**, 3788 (2003); R. A. Puglisi, S. Lombardo, G. Ammendola, G. Nicota, and C. Gerardi, *Mater. Sci. Eng., C* **23**, 1047 (2003).
- ⁶⁰K. Nishiguchi and S. Oda, *J. Appl. Phys.* **88**, 4186 (2000).
- ⁶¹M. R. Reshotko and I. Balberg, *Appl. Phys. Lett.* **78**, 763 (2001).